The Thermal Conductivity of Nylon 6/Clay Nanocomposites

Hu Zhou, Shimin Zhang, Mingshu Yang

Beijing National Laboratory for Molecular Sciences (BNLMS), Key Laboratory of Engineering Plastics, Institute of Chemistry, Chinese Academy of Sciences, Beijing 100080, People's Republic of China

Received 16 September 2007; accepted 28 December 2007
DOI 10.1002/app.27984
Published online 12 March 2008 in Wiley InterScience (www.interscience.wiley.com).

ABSTRACT: Nylon 6/clay nanocomposites (NCNs) of different clay loadings are prepared by melt compounding. The effects of clay loading and dispersion on the thermal conductivity of NCNs are investigated using XRD, TEM, DSC, and POM. The results show that the thermal conductivity of the exfoliated NCNs decreases with an increase of clay content; but the thermal conductivity of the intercalated NCNs does not decrease, indeed, it increase markedly at high clay content. Such results observed in the exfoliated NCNs are opposite to the expectation of the classic Maxwell thermal conduction model. The further investigations indicate that such decrease observed in the exfoliated NCNs is due mainly to the exfoliation of clay layers. © 2008 Wiley Periodicals, Inc. J Appl Polym Sci 108: 3822–3827, 2008

Key words: nylon 6/clay nanocomposites; thermal conductivity

INTRODUCTION

Polymer/clay nanocomposites (PCNs) are a new emerging class of organic-inorganic hybrid materials, which contain nanoscale dispersed clay fillers of sheet-like structural blocks with thickness of 1 nm, diameter from 10 to 1000 nm. In the past decades, PCNs have received widespread attention for their intriguing structures and properties.[1] With much less content of clay (layered silicates such as montmorillonite, saponite, laponite, hectorite, etc.,) than comparable glass- or mineral-reinforced polymers, PCNs exhibit physical and mechanical properties significantly different from their conventional counterparts. They have high modulus, high strength, high heat distortion temperature, good gas/vapor barrier properties, and flame retardancy with as little as 5 wt % clay content.[2–6] It is generally believed that the improvements of their barrier and other mechanical properties are mainly caused by the high aspect ratio (10–1000) or large surface area of exfoliated clay layers and the strong interfacial interaction between the clay layers and the polymer matrix.[1,7]

Recently, a few investigations have devoted attention to the thermal conductivity of PCNs.[8,9] Lee et al.[8,10] studied the thermal conductivity of the exfoliated nanocomposites prepared by melt mixing maleated polyethylene and laponite (mPE/clay), and observed that the thermal conductivity decreased with an increase of clay content. Previously, Yao et al.[9] also found a similar result in polyurethane/clay nanocomposites of low clay loadings (PU/clay). Generally, the thermal conductivity of clay is higher than one of polymers, since the thermal conductivity of clay is about 1 Wm^{-1} K^{-1},[11] while one of common polymers is less than 0.5 Wm^{-1} K^{-1}.[12] Thus, according to the classic Maxwell thermal conduction model,[13] the presence of clay will result in increasing the thermal conductivity of PCNs. But, the observed results of mPE/clay and low clay loading PU/clay are the opposite of this expectation. Obviously, there are some unknown factors present which result in decreasing the thermal conductivity of PCNs. However, the investigations of Lee et al.[8] and Yao et al.[9] did not give a specific explanation of the observed results. In fact, it is not certain yet about the origin of such results.

The motivation of this work is to explore the origin of such results in the PCNs. The thermal conductivity of Nylon 6/clay nanocomposites (NCNs) is investigated as a model system, because NCNs with different dispersion states of clay could be prepared easily. NCNs of different clay loadings are prepared by melt compounding, which is described in our previous work.[14,15] The thermal conductivity of NCNs is determined by using the method which is described in the literature.[16–20] The dispersion states of clay in NCNs are characterized by transmission electron microscopy (TEM) and X-ray diffraction (XRD). Moreover, DSC, XRD, and polarized optical

Correspondence to: M. S. Yang (yms@iccas.ac.cn).
Contract grant sponsor: Major Basic Research Projects of China; contract grant number: 003CB615600.

TABLE I
Thermal Properties of Nylon 6 and NCNs

Sample	Clay content (wt %)	Melting peak (°C)	Heat of fusion (J g^{-1})	Crystallinity[a] (%)
Nylon 6	0	211.9/220.3	64.2	33.8
Nylon 6/Na-MMT-3	2.4	210.8/219.7	56.6	29.8
Nylon 6/Na-MMT-20	17.7	210.2/218.7	58.6	30.8
Nylon 6/OMMT-1	0.63	211.4/220.8	63.3	33.3
Nylon 6/OMMT-3	2.9	210.6/219.4	55.6	29.3
Nylon 6/OMMT-5	5.4	210.7/219.7	59.4	31.3
Nylon 6/OMMT-10	11.1	209.7/218.5	61.5	32.4
Nylon 6/OMMT-20	18.6	208.0/216.7	61.2	32.2

[a] The crystallinity of various nylon 6 systems is calculated from the enthalpy evolved during melt based on the heating scans, and the involved formula can be found in the literature.[14]

microscope (POM) are used to provide detailed information on the crystalline phase of pure nylon 6 and NCNs.

EXPERIMENTAL

Materials

Nylon 6 resins (Capron®8200 NL) with a density of 1.13 g/cm^3 is kindly supplied by Honeywell Nylon System (China) and used after drying under vacuum at 80°C for 8 h. Sodium montmorillonite (Na-MMT), with a cation-exchange capacity of 85 mequiv/100 g, is purchased from Zhangjiakou Qinghe Chemical Plant Co. (China). Octadecyl diethanolamine is supplied by Shanghai Jinshan Chemical Co. (China) and used after protonized by hydrochloric acid. Other reagents are of commercial products and used as received.

The organo-montmorillonite (OMMT) is prepared by cation-exchange reaction with octadecyl diethanolamine salt formed by protonizing the amine. The experimental process of preparing OMMT is described in detail in our previous work.[14,15] The yielded OMMT is dried under vacuum at 80°C for 8 h and then ground to fine powders with diameters of 40–70 μm.

Preparation of samples

NCNs are prepared with a twin-screw extruder (Nanjing Rubber and Plastics Machinery Plant, SHJ-30, China) with a 30-mm diameter and an L/D ratio of 23. The extrudates are palletized at the die exit, dried, and injection-molded into 4-mm thick standard Izod bars (ASTM D256) with an injection-molding machine (SZ-68/400, Chende Plastic Machinery, China) at mold temperature of 60°C. The detailed process of preparing NCNs and the standard Izod bars is described in our previous work.[14,15] The exact amount of clay in NCNs is determined by placing pre-dried extruded pellets in a furnace at 900°C for 45 min and weighing the residual ash.[21] The results are corrected for loss of structural water contained in the clay,[21] as shown in Table I.

Specimens with approximate dimensions of 5.0 × 5.0 × 1.0 mm^3 are cut from the core region of the injection-molded Izod bars along the injection direction after they are annealed under vacuum at 80°C for 12 h. The surfaces of specimens are polished with 2000-grit SiC sandpaper before determining the thermal conductivity.

Characterization

XRD patterns are obtained using a Rigaku D/max 2400 diffractometer (40 kV, 200 mA; Cu Kα, λ = 0.154 nm; reflection mode). XRD scans are performed on the specimens prepared for determining the thermal conductivity, as well as on Na-MMT and OMMT powder, at ambient temperature with a 2θ range between 1° and 40°, at a scanning rate of 4°/min and a scanning step of 0.02°.

DSC analyses are carried out on a Perkin–Elmer DSC-7 differential scanning calorimeter thermal analyzer in a nitrogen environment. The sliced samples (∼ 5 mg, and cut from the core region of injection-molded Izod bars) are heated at a rate of 20°C/min from 50 to 250°C.

The morphology of the NCNs is investigated by a Hitachi H-800 transmission electron microscope apparatus at an acceleration voltage of 200 kV. Ultrathin sections are obtained by cryogenic ultramicrotoming the injection-molded samples along the injection direction.

The crystalline phase morphology of nylon 6 and NCNs is observed using a Leica DM LP-MP30 POM. The slices with a thickness of ∼ 30 μm are sliced from the core region of injection-molded Izod bars along the injection direction using a Leica RM2155 microtome.

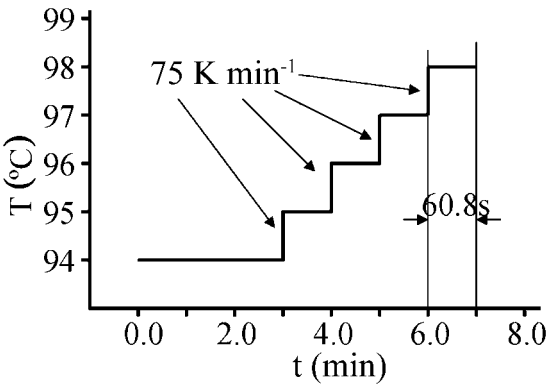

Figure 1 Temperature-time program, consisting of 1K steps in temperature and 60 s isotherms. Temperature steps are programmed as short heating segments with 75 K min^{-1} heat rate.

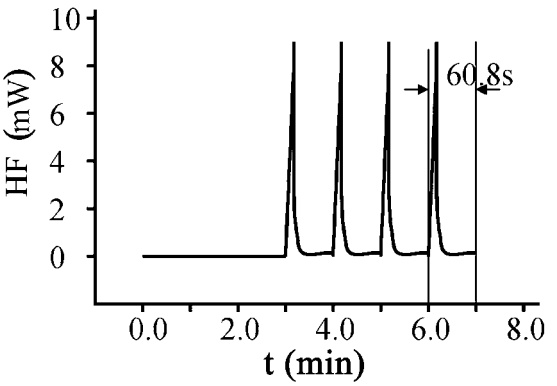

Figure 2 An example of measured heat flow rate (HF) versus time, corresponding to the temperature-time program shown in Figure 1. The last peak was taken for further data evaluation.

Determining the thermal conductivity

The thermal conductivity of nylon 6 and NCNs is determined by using the method which is described in the literature.[16–20] Its principle is based on the heat capacity spectra of three specimens obtained in two different situations: equilibrium and nonequilibrium thermal conditions. The thermal equilibrium measurement is achieved by using two aluminum disks, a thin (<0.5 mm) and a thick (>1.0 mm), for dynamic calibration of the instrument. For the nonequilibrium measurement, a sample disk (>1.0 mm) is placed over DSC furnace so that the temperature oscillation can be applied only to one side of the test specimen, producing a temperature gradient across the specimen. To obtain the heat capacity spectra, it is necessary to use the technique of the single step in the program temperature. The heat capacity spectra obtained in both situations along with some geometric and experimental parameters is used to determine the thermal conductivity of the samples. The theory and the derivation of the equations involved in this method are discussed in detailed by Merzlyakov and Schick.[16–19] The experimental procedure and mathematical treatment are given in the Internet.[20]

In this work, the measurements comply completely with the experimental procedure provided in the Internet,[20] and are performed on a Perkin-Elmer Diamond DSC differential scanning calorimeter thermal analyzer. Purge gas is nitrogen with gas flow of 20 mL min^{-1}. Temperature-time program shown in Figure 1 is used to generate the spectrum of apparent heat capacity. Initial isotherm of 3 min is added to check whether heat flow drifting at steady state is remarkable. Corresponding heat flow rate after empty furnace correction is shown in Figure 2 (we do not use a pan, and hence subtract the heat flow measured with an empty furnace). The last step is evaluated and the corresponding temperature is 98°C. We take into consideration up to five frequencies $\omega_k = k\omega_0$, $k = \{1, 2, 3, 4, 5\}$, $\omega_0 = 2\pi/t_p$ and $t_p = 60.8$ s.

RESULTS

The XRD profiles of NCNs and two kinds of clay are shown in Figure 3. The (001) plane peak of Na-MMT is around 7.02°, and the broad peak of OMMT is about 4.44°, showing the intercalation of quaternary ammonium cation in the clay. In nylon 6/Na-MMT nanocomposites, the peaks are still present and only shift toward the lower 2θ, indicating that Na-MMT is intercalated by nylon 6 molecules. In nylon 6/OMMT nanocomposites, any reflection peak is not visible up to 5.4 wt % of clay, which indicates that OMMT is potentially exfoliated, but the reflection peaks are still present when the clay content reaches 10 wt %, which shows that the intercalation structure

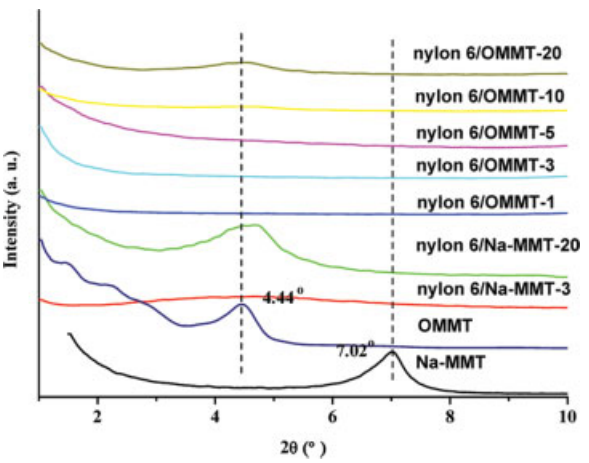

Figure 3 XRD patterns of Na-MMT, OMMT, and NCNs. [Color figure can be viewed in the online issue, which is available at www.interscience.wiley.com.]

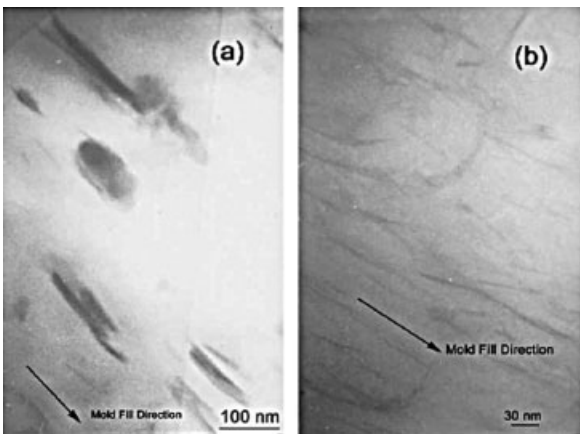

Figure 4 TEM images of NCNs: (a) nylon 6/Na-MMT-3 and (b) nylon 6/OMMT-3.

is formed again. TEM is used to further confirm the dispersion states of Na-MMT and OMMT in nylon 6 matrix. Figure 4(a,b) shows that Na-MMT is intercalated as stacks and agglomerates of large size in nylon 6/Na-MMT-3, and OMMT is almost fully exfoliated to individual clay layers in nylon 6/OMMT-3. The dispersion states of clay of different NCNs are summarized in Table II.

DSC melting curves of nylon 6 and NCNs are plotted in Figure 5, and related thermal properties derived from the DSC thermograms are summarized in Table I. Figure 5 shows that the melting behaviors of pure nylon 6 and various NCNs are similar, though the sub-T_m transitions are more obvious with the increase of the clay content, which is possibly caused by the imperfect crystals[14,15,21] or the γ crystalline phase.[22] As shown in Table I, the crystalline contents of various NCNs are slightly lower than that of pure nylon 6, and moreover the melting peak temperatures of pure nylon 6 and low clay loading NCNs (<10 wt %) are almost same, while the melting peaks shift toward the lower temperature in high clay loading NCNs (≥10 wt %), which is potentially related to the imperfect crystals.

TABLE II
The Thermal Conductivity and Clay Dispersion State in the Samples

Sample	K^a (Wm^{-1} K^{-1})	Dispersion
Nylon 6	0.28	–
Nylon 6/Na-MMT-3	0.28	intercalated
Nylon 6/Na-MMT-20	0.35	intercalated
Nylon 6/OMMT-1	0.27	exfoliated
Nylon 6/OMMT-3	0.25	exfoliated
Nylon 6/OMMT-5	0.24	exfoliated
Nylon 6/OMMT-10	0.28	intercalated/ exfoliated
Nylon 6/OMMT-20	0.45	intercalated

[a] The thermal conductivity is obtained at 98°C, and its uncertainty is ±10%.

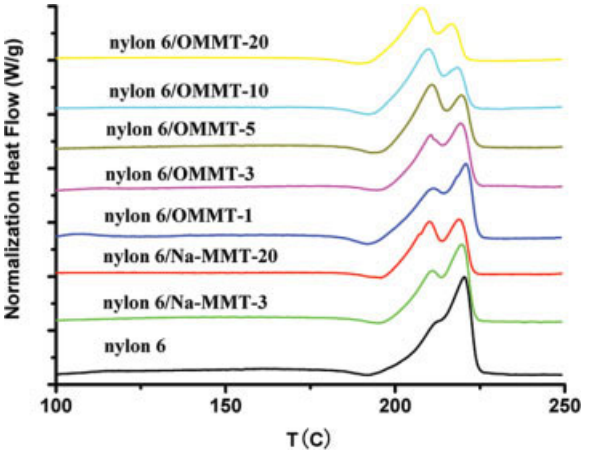

Figure 5 Melting behavior thermograms of nylon 6 and NCNs. [Color figure can be viewed in the online issue, which is available at www.interscience.wiley.com.]

The crystalline phase morphology of various nylon 6 systems is observed using POM, as shown in Figure 6. It is observed that spherical crystal grains are dispersed randomly in the matrix for three nylon 6 systems. Moreover, the coarse analysis of the polarized optical microscopy images shows that spherical crystal grains of three nylon 6 systems do not exhibit a substantial difference in the size. Although the investigations[1,4] show that the presence of clay results in decreasing the size of crystal grains in NCNs due to the nucleation effect, the nucleation effect of clay has a small influence on the size of crystal grains in our work, which is possibly due to the fast cooling used in the processing of the standard Izod bars. In addition, the obvious characteristic of the orientation of molecule chains and crystal grains is not observed between the cross polarizers, as shown in Figure 6.

As shown in Table II, the thermal conductivity of exfoliated NCNs is lower than that of nylon 6, and moreover decreases with the increase of the clay content; but the thermal conductivity of intercalated NCNs does not reveal decrease, indeed, it increase markedly at high clay content. The thermal conductivity of clay is about 1 Wm^{-1} K^{-1},[11] which is higher than that of nylon 6. Thus, according to the classic Maxwell thermal conduction model,[13] the presence of clay will result in an increase of the thermal conductivity of NCNs. However, the observed results in the exfoliated NCNs are opposite to this expectation. Previously, the investigations on the thermal conductivity of mPE/clay and PU/clay also reported the similar results.[8,9] Obviously, there are the unknown factors which result in decreasing the thermal conductivity of exfoliated NCNs; however, it is not certain yet about the unknown factors. We speculate that such results are possibly related to the dispersion state of clay as well as the orientation and

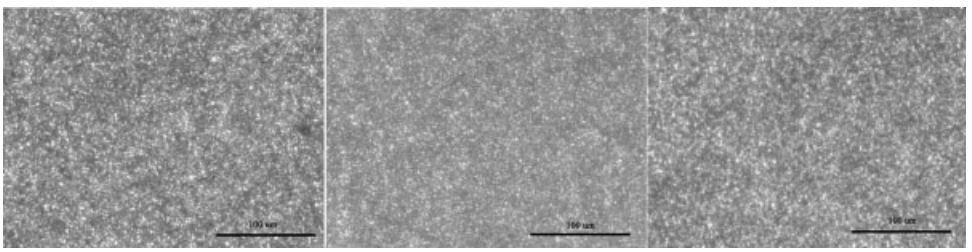

Figure 6 Polarized optical microscopy images of three nylon 6 systems. From left to right: nylon 6, nylon 6/Na-MMT-3, and nylon 6/OMMT-3.

crystallinity of molecules. Later, it will be discussed in detail.

DISCUSSION

It is well known that three essential aspects of the thermal conductivity of polymers are the temperature dependence, the crystallinity dependence, and the orientation effect.[23–30] In his review, Choy gives a particular description of the effect of temperature, crystallinity and orientation on the thermal conductivity of polymers.[23] Generally, crystallization results in increasing the thermal conductivity of polymers, and orientation has different influences on the thermal conductivity of polymers: increasing the thermal conductivity along the orientation direction and decreasing the thermal conductivity perpendicular to the orientation direction.

In our work, the effect of temperature on the thermal conductivity of the nylon 6 systems is not considered due to determining the thermal conductivity at the same temperature. Moreover, the results of POM show that the orientation of molecular chains and crystal is absent in the nylon 6 systems. Hence, the effect of orientation on the thermal conductivity of the nylon 6 systems may be ignored. In this way, the left factors are crystallinity and clay, which can result in decreasing or increasing the thermal conductivity of NCNs.

Our investigations show that nylon 6 and NCNs do not differ substantially in the crystalline content, and the size and dispersion of spherical crystal grains as well as the melting behavior. Thus, a thermal conduction model of semicrystalline polymers presented by Choy and Young[30] can be applied to quite accurately evaluate the effect of crystallinity. The thermal conductivity of semicrystalline polymers is given by this model as:

$$\frac{k-k_a}{k+2k_a} \cong X\left[\frac{2}{3}\frac{k_\perp-1}{k_\perp+2}+\frac{1}{3}\right] \quad (1)$$

where k is the thermal conductivity of semicrystalline polymers; k_a is the thermal conductivity of the amorphous region; $k_\perp = k_{c\perp}/k_a$; and $k_{c\perp}$ is the thermal conductivity perpendicular to the chain direction of a crystallite. Generally, $k_\perp$ is close to one, and hence $k_\perp = 1$ is used in a rough calculation. The results show that the decrease of the crystalline content by 10% will result in only decreasing the thermal conductivity by about 4%.

The experiments observe that the crystalline content decreases by 7.4% in nylon 6/OMMT-5, which will result in decreasing the thermal conductivity by about 3% in nylon 6/OMMT-5 according to eq. (1). However, the experiments observe that the thermal conductivity of nylon 6/OMMT-5 decreases by about 14%. Moreover, the rough calculation shows that the decrease of the thermal conductivity observed in all the exfoliated NCNs are larger than one caused by the decrease of the crystalline content. On the other hand, clay as the stacks and agglomerates can result in increasing the thermal conductivity of NCNs, which has been observed in the high loading NCNs. Hence, it can be thought that such results in the exfoliated NCNs are due mainly to the exfoliation of clay layers.

The exfoliation of clay layers dramatically increases the surface of clay, resulting in larger interfacial thermal resistance[31–33]; on the other hand, it results in decreasing the thermal conductivity of clay self by one to three orders of magnitude due to the size effect which has been demonstrated by the investigations on thermal conduction of nanostructures.[34–36] These two factors will result in decreasing the thermal conductivity of the exfoliated NCNs. On the contrary, the effect of the size effect and interface effect is smaller in the high loading NCNs due to large size of clay stacks and agglomerates. In this instance, the classic Maxwell thermal conduction model can be used to predict the thermal conductivity of the high loading NCNs.[13,37,38] As a result, it is found that the calculating values are consistent in the trend with the experimental values.

CONCLUSIONS

The thermal conductivity of nylon 6 and NCNs is measured using the method described in references.[12–17] The results indicate the thermal conductivity

of exfoliated NCNs is lower than that of nylon 6, and moreover decreases with an increase of the clay content; but the thermal conductivity of intercalated NCNs does not reveal decrease, indeed, it increase markedly at high clay content. Such results observed in the exfoliated NCNs are the opposite of the expectation from the classic Maxwell thermal conduction model.

The further investigations reveal that such unusual decrease of the thermal conductivity in the exfoliated NCNs is due mainly to the exfoliation of clay, and that the increase of the thermal conductivity in the high loading NCNs is due to the presence of large clay stacks and agglomerates. The exfoliation of clay layers not only dramatically increases the surface of clay, resulting in larger interfacial thermal resistance, but also results in a decrease of the thermal conductivity of clay by one to three orders of magnitude due to the size effect. These two factors will result in decreasing the thermal conductivity of the exfoliated NCNs. However, the influence of the size effect and interface effect is very small in the high loading NCNs due to large size of clay stacks and agglomerates. Hence, the presence of clay will result in increasing the thermal conductivity in the high loading NCNs, since the bulk clay exhibits a higher thermal conductivity than nylon 6.

The authors thank Doc. S. Xie for helping us prepare nylon 6/clay nanocomposites, and also acknowledge the help from G. Li in determining the thermal conductivity.

References

1. Pinnavaia, T. J.; Beall, G. W. Polymer-Clay Nanocomposites; Wiley: New York, 2000.
2. Usuki, A.; Kojima, Y.; Kawasumi, M.; Okada, A.; Fukushima, Y.; Kurauchi, T.; Kamigaito O. J Mater Res 1993, 8, 1179.
3. Kojima, Y.; Usuki, A.; Kawasumi, M.; Okada, A.; Fukushima, Y.; Kurauchi, T.; Kamigaito, O. J Mater Res 1993, 8, 1185.
4. Liu, L.; Qi, Z.; Zhu, X. J Appl Polym Sci 1999, 71, 1133.
5. Chaiko, D. J.; Leyva, A. A. Chem Mater 2005, 17, 13.
6. Gilman, J. W.; Jackson, C. L.; Morgan, A. B.; Harris, R., Jr.; Manias, E.; Giannelis, E. P.; Wuthenow, M.; Hilton, D.; Phillips, S. H. Chem Mater 2000, 12, 1866.
7. Rao, Y.; Pochan, J. M. Macromolecules 2007, 40, 290.
8. Lee, S. H.; Kim, J. E.; Song, H. H.; Kim, S. W. Int J Thermophys 2004, 25, 1585.
9. Yao, K. J.; Song, M.; Hourston, D. J.; Luo, D. Z. Polymer 2002, 43, 1017.
10. Wang, K. H.; Choi, M. H.; Koo, C. M.; Xu, M.; Chung, I. J.; Jang, M. C.; Choi, S. W.; Song, H. H. J Polym Sci, Part B: Polym Phys 2002, 40, 1454.
11. Abu-Hamdeh, N. H.; Reeder, R. C. Soil Sci Soc Am J 2000, 64, 1285; and references therein.
12. Dean, J. A. Lange's Handbook of Chemistry, 15th ed.; McGraw-Hill: New York, 1999.
13. Maxwell, J. C. A Treatise on Electricity and Magnetism, 3rd ed.; Dover: New York, 1954.
14. Xie, S.; Zhang, S.; Liu, H.; Chen, G.; Feng, M.; Qin, H.; Wang, F.; Yang, M. Polymer 2005, 46, 5417.
15. Xie, S.; Zhang, S.; Zhao, B.; Qin, H.; Wang, F.; Yang, M. Polym Int 2005, 54, 1673.
16. Merzlyakov, M.; Schick, C. Thermochim Acta 2001, 377, 183.
17. Merzlyakov, M.; Schick, C. Thermochim Acta 2001, 380, 5.
18. Merzlyakov, M.; Schick, C. Thermochim Acta 1999, 330, 65.
19. Merzlyakov, M.; Schick, C. Thermochim Acta 2001, 377, 193.
20. See: http://www.uni-rostock.de/fakult/manafak/physik/poly/
21. Fornes, T. D.; Yoon, P. J.; Keskkula, H.; Paul, D. R. Polymer 2001, 42, 9929.
22. Hu, X.; Zhao, X. Polymer 2004, 45, 3819.
23. Choy, C. L. Polymer 1977, 18, 984.
24. Choy, C. L. J Phys C: Solid State Phys 1977, 10, 169.
25. Choy, C. L.; Luk, W. H.; Chen, F. C. Polymer 1978, 19, 155.
26. Choy, C. L.; Chen, F. C.; Luk, W. H. J Polym Sci Polym Phys Ed 1980, 18, 1187.
27. Choy, C. L.; Ong, E. L.; Chen, F. C. J Appl Polym Sci 1981, 26, 2325.
28. Choy, C. L.; Wong, S. P.; Young, K. J Polym Sci Polym Phys Ed 1985, 23, 1495.
29. Finlayson, D. M.; Mason, P. J. J Phys C: Solid State Phys 1985, 18, 1791.
30. Choy, C. L.; Young, K. Polymer 1977, 18, 769.
31. Benveniste, Y. J Appl Phys 1987, 61, 2840.
32. Hasselman, D. P. H.; Johnson, L. E. J Compos Mater 1987, 21, 508.
33. Nan, C. W.; Birringer, R.; Clarke, D. R.; Gleiter, H. J Appl Phys 1997, 81, 6692.
34. Majumdar, A. ASME J Heat Trans 1993, 115, 7.
35. Chen, G. ASME J heat transfer 1997, 119, 220.
36. Chen, G. ASME J Heat Transfer 1996, 118, 539.
37. Chen, G. Int J Therm Sci 2000, 39, 471.
38. Chen, G. J Nanopart Res 2000, 2, 199.